Check for updates

Liquid-crystal-based magnetically tunable terahertz achromatic quarter-wave plate

CHO-FAN HSIEH,[1,6] CHAN-SHAN YANG,[2,3,6,7] FANG-CIH SHIH,[4] RU-PIN PAN,[5] AND CI-LING PAN[4,8]

[1]Photovoltaic Metrology laboratory, Center for Measurement Standards, Industrial Technology Research Institute, Hsinchu 31057, Taiwan
[2]Institute of Electro-Optical Science and Technology, National Taiwan Normal University, Taipei 11677, Taiwan
[3]Undergraduate Program of Electro-Optical Engineering, National Taiwan Normal University, Taipei 11677, Taiwan
[4]Department of Physics, National Tsing Hua University, Hsinchu 30013, Taiwan
[5]Department of Electrophysics, National Chiao Tung University, Hsinchu 30010, Taiwan
[6]These authors contributed equally to this work
[7]csyang@ntnu.edu.tw
[8]clpan@phys.nthu.edu.tw

Abstract: Development of the wideband and tunable quasi-optic terahertz (THz) components is in high demand. In this work, we demonstrate a tunable achromatic quarter-wave plate (AQWP) for the THz frequency range. The phase retardation of this device can be set at $90° \pm 9°$ from 0.20 to 0.50 THz. The operation range from 0.20 to 0.50 THz can be tuned to from 0.30 to 0.70 THz by introducing three nematic liquid crystals phase retarders, of which the birefringence can be magnetically tuned. The frequency-dependent phase retardation is in good agreement with theoretical predictions.

1. Introduction

Wave plates are essential for modulating the polarization states of light. The basic wave plate is designed to work at a particular wavelength. Therefore, achromatic wave plate (AWP) with a broad operating wavelength range is required for many applications. Several types of achromatic phase retarders have been demonstrated so far. Mainly, these are for the visible and near-infrared (NIR) wavelength range [1–5]. The terahertz (THz) technology and science have been in full swing for over two decades [6]. These research and developments urgently need the quasi-optic THz components, such as polarizers [7], phase shifters [8–11], phase gratings [12–15], and wave plates [16–19]. Masson et al. reported an achromatic quarter-wave plate (AQWP) in the THz frequency range by using six or more pieces of birefringent crystalline quartz plates [17]. Owing to the number of quartz plates with precise thickness needed, the fabrication of this kind of AWP is very complicated and bulky. Recently, Zhang et al. also demonstrated an wideband AQWP using silicon grating [16]. However, both of these designs cannot adjust the achromatic range. Nematic liquid crystals (LCs) have been used in AWPs because its birefringence is relatively high and can be controlled electrically or magnetically. Previously, our group demonstrated the feasibility of reducing pulse broadening by applying the achromatic half wave plate and AQWP made of two and three LCs cells stacked together [3]. In the past years, we have also demonstrated several THz phase shifters based on magnetically or electrically controlled birefringence in nematic LCs [8–11,20]. Most of these devices are capable of being designed for more than 360° of phase shift around 1 THz by increasing the thickness of LCs cell [10,20]. Recently, electrically tunable 2π THz phase shifters based on a sandwiched LC cell with indium-tin-oxide nanowhiskers as transparent electrodes have been well demonstrated [10]. Further, the magnetically tunable 2π LCs THz phase shifter can be operated over a broad range near room temperature [20].

As described above, by picking up low-loss transparent electrodes which are extremely rare in the THz frequency range [8,10,11,19], the electrically tunable achromatic wave plate can be demonstrated. The advantage of applying the magnetic fields to tune LCs is without the requisite of transparent electrodes.

In this work, we proposed and demonstrated a LCs-based THz AQWP, of which the phase retardation can be tuned by changing the effective refractive index of LCs. The device consists of a standard half-wave plate and two standard third-wave plates. The critical concept is the partial cancellation of the change of retardation with frequency from each wave plate.

2. Experimental method

To shift THz operation range, we extended the design to a combination of three magnetically controlled LC phase retarders. Nematic LCs E7 are reasonably transparent in the THz range [21], and it also exhibits large birefringence. In THz frequency range, the ordinary and extraordinary refractive indices of E7 are n_o = 1.58 and n_e = 1.71, respectively, and the corresponding imaginary indices are κ_o (0.01) to κ_e (0.007) [21].

The LC-based achromatic wave plate has three elements, TR_A, TR_B and TR_C, which are tunable retarders (TRs) and shown in Fig. 1. Each TR consists of a pair of rotatable permanent magnets and a homeotropically aligned LC cell. The LC cell in the TR was constructed with two fused silica substrates and filled with nematic LCs, E7 (Merck). The substrates of LC cells were coated with N, N-dimethyl-n-octadecyl-3-aminopropyltrimethoxysilyl chloride (DMOAP) for homeotropic alignment [22]. Thicknesses of LC layers in TR_A, TR_B and TR_C were d_A = 2.56 mm, d_B = 3.86 mm, and d_C = 2.56 mm, controlled by Teflon spacers. Besides, the thickness of fused silica is around 1mm. The threshold field required to reorient LC molecules with the magnetic field is less than 0.004 Tesla [23]. The maximum magnetic field at cell position in the rotary permanent magnets (sintered Nd-Fe-B) is 0.25 Tesla. Sufficiently large magnetic field is applied for stable homogeneous alignment of LC molecules in the thick LC cell. The rotation axis of rotary magnets is perpendicular to the propagation direction of the THz wave and has an azimuthal angle ρ_i with respect to the normal axis of the table (ρ_A = 0°, ρ_B = 20° and ρ_C = 0°). So TR_A, TR_B, and TR_C are used to achieve the desired variable phase retardation, $\Gamma_A(\theta)$, $\Gamma_B(\theta)$ and $\Gamma_C(\theta)$, where θ is defined as the angle between the director of LC molecules and the polarization direction of electromagnetic wave. The TRs were placed between a pair of wire-grid polarizers (Specac, No. GS57204). We set the polarizer at fixed azimuthal angle ρ_p = −75°, it made the optic axis of achromatic quarter wave plate has 45° with respect to the polarization direction of THz wave in our photoconductive-antenna (PCA)-based transmission-type THz time-domain spectroscopy (THz-TDS) which has been described well in our previous works for characterization of the devices and materials in the THz frequency range [24]. The schematic cartoon of THz emitter and detector is also shown in Fig. 1. The THz-TDS was always purged with dry nitrogen, so the relative humidity was maintained at 5.0 ± 0.5%. In this work, the inclination angles θ = 0° and θ = 30° for all TRs were demonstrated. The corresponding birefringence of LCs is 0.13 and 0.095, respectively. By rotating the magnetic field, the operation frequency range was shifted for that corresponding retardations were equal to quarter wave.

Basically, the purpose to design an THz AQWP can be regarded as finding combinations of retarders causing paths from a linearly polarization state (a fixed point on the equator of the sphere) to a circular polarization state (north of south pole of the sphere) on the Poincaré sphere over a wide THz frequency range. The theoretical model to achieve the goal is based on the analysis of Jones matrices with the phase difference equation, and retrieved total phase retardation from matrices. Each LC wave plate is described by its corresponding Jones matrix J_i (i = A, B and C) [23],

$$J_i(\Gamma_i,\psi_i) = R\begin{pmatrix}\cos\psi & -\sin\psi \\ \sin\psi & \cos\psi\end{pmatrix}\begin{pmatrix}e^{-i\Gamma/2} & 0 \\ 0 & e^{i\Gamma/2}\end{pmatrix}R\begin{pmatrix}\cos\psi & \sin\psi \\ -\sin\psi & \cos\psi\end{pmatrix}$$

$$= \begin{bmatrix}\cos\dfrac{\Gamma_i}{2}-i\cos 2\psi_i\sin\dfrac{\Gamma_i}{2} & i\sin 2\psi_i\sin\dfrac{\Gamma_i}{2} \\ i\sin 2\psi_i\sin\dfrac{\Gamma_i}{2} & \cos\dfrac{\Gamma_i}{2}+i\cos 2\psi_i\sin\dfrac{\Gamma_i}{2}\end{bmatrix} \tag{1}$$

which the phase retardation Γ_i and the orientation angle ψ_i with respect to the optical axis are two key parameters in Eq. (1). The total Jones matrix of achromatic wave plate is given by [23], and it can be written into

$$J = \prod_i J_i = \begin{bmatrix} A & B \\ -B* & A* \end{bmatrix}, \tag{2}$$

where the A, B, $-B^*$, and A^* correspond to the matrix components. The total resulting retardation is obtained by

$$\tan^2\frac{\Gamma}{2} = \frac{|\operatorname{Im}A|^2+|\operatorname{Im}B|^2}{|\operatorname{Re}A|^2+|\operatorname{Re}B|^2} \tag{3}$$

For LC wave plates, the inclination angle, θ, is defined as the angle between the director of LC molecules and the polarization direction of electromagnetic wave. The orientation of the LC molecules, which can be described by the angle θ, is proportional to the effective refractive index of LCs [8]. The phase retardation, $\Gamma_i(\theta)$, due to magnetically controlled birefringence is given by

$$\Gamma_i(\theta) = \int_0^d \frac{2\pi f}{c}\Delta n_i(\theta,z)dz, \tag{4}$$

where d is the thickness of LC layer, Δn_i is the change of effective birefringence, f is the frequency of the THz waves and c is the speed of light in vacuum. If the magnetic field is strong enough, LC molecules can be reoriented and parallel to the direction of the magnetic field. The phase retardation, $\Gamma_i(\theta)$, in Eq. (4) can then be re-written as

$$\Gamma_i(\theta) = 2\pi d\frac{f}{c}\left\{\left[\frac{\cos^2(\theta)}{n_e^2}+\frac{\sin^2(\theta)}{n_o^2}\right]^{-\frac{1}{2}}-n_o\right\}, \tag{5}$$

where n_o and n_e are the ordinary and extra-ordinary refractive indices of the LC. As expected, the tunable operation range of achromatic quarter wave plate is achieved by using three magnetically controlled LC retarders.
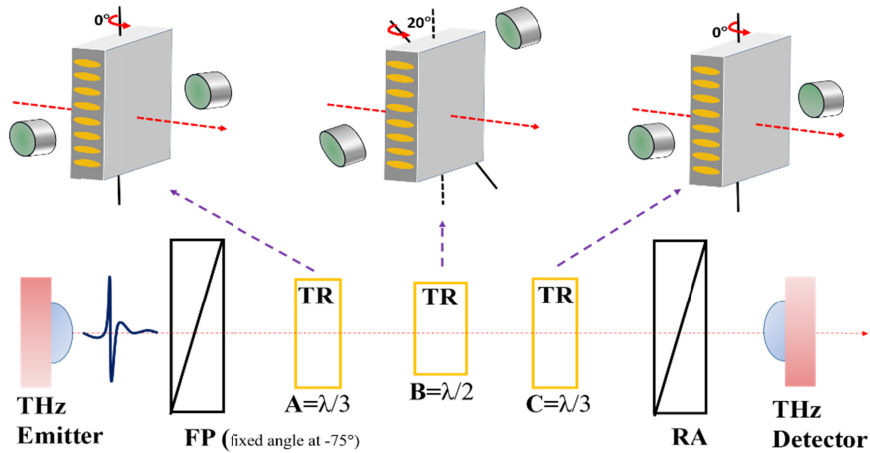
Fig. 1. The LC-based achromatic wave plate has three elements, A, B and C. Each tunable retarder (TR) consists of a pair of rotatable permanent magnets and a homeotropically aligned LC cell. The FP and RA represent polarizer with fixed angle at −75° and rotating analyzer, respectively. Thicknesses of LC layers in TR_A, TR_B and TR_C were d_A = 2.56 mm, d_B = 3.86 mm, and d_C = 2.56 mm, respectively.

The PCA-based THz-TDS only can detect the linear polarized THz field. To measure the retardation of LC based THz quarter wave plate, we introduced a new method of the ellipsometry by rotating wire grid analyzer [17]. This technique allows determination of the retardation of the wave plate without rotating or moving the detector. A horizontal linearly polarized THz wave is sent through the wave plate to be investigated. The final exiting electric field E_{final} carries out information on the wave plate as follows

$$E_{final}(\phi) = \begin{bmatrix} 1 & 0 \\ 0 & 0 \end{bmatrix} \begin{bmatrix} \cos^2\phi & \sin\phi\cos\phi \\ \sin\phi\cos\phi & \sin^2\phi \end{bmatrix} \begin{bmatrix} \cos\dfrac{\Gamma}{2} - i\cos 2\psi\sin\dfrac{\Gamma}{2} & i\sin 2\psi\sin\dfrac{\Gamma}{2} \\ i\sin 2\psi\sin\dfrac{\Gamma}{2} & \cos\dfrac{\Gamma}{2} + i\cos 2\psi\sin\dfrac{\Gamma}{2} \end{bmatrix}$$

$$\begin{bmatrix} \cos^2 15° & -\sin 15°\cos 15° \\ -\sin 15°\cos 15° & \sin^2 15° \end{bmatrix} \begin{bmatrix} 1 \\ 0 \end{bmatrix} \quad (6)$$

where ϕ is the angle between the analyzer with respect to the detecting direction of antenna, and $P_{exp}(\phi) = (E_{final}(\phi))^2$ is the power of THz wave which can be obtained from experimental measurement. We can extract the phase retardation of our device by using Eq. (6).

3. Experimental results

The signal has been recorded in steps of 30° of the analyzer angle ϕ, leading to 24 times. The temporal waveforms of the THz pulse transmitted through the tunable AQWP with the E7 LCs layer aligned at magnetic inclination angle $\theta = 0°$ with different rotating angles ϕ are shown in Fig. 2. The transmitted amplitude of THz fields exhibit symmetry with respective to $\theta = 0°$ in time domain, because the most of transmitted broadband THz signals are circular polarized and only horizontal polarization of THz wave can be detected by photoconductive antenna. Then, power spectral data can be achieved by using fast Fourier transform of the temporal data. Here, the cases of 0° in black with the solid line and 180° in black with the dashed line should be the same condition, so that curves are consistent with each other well.
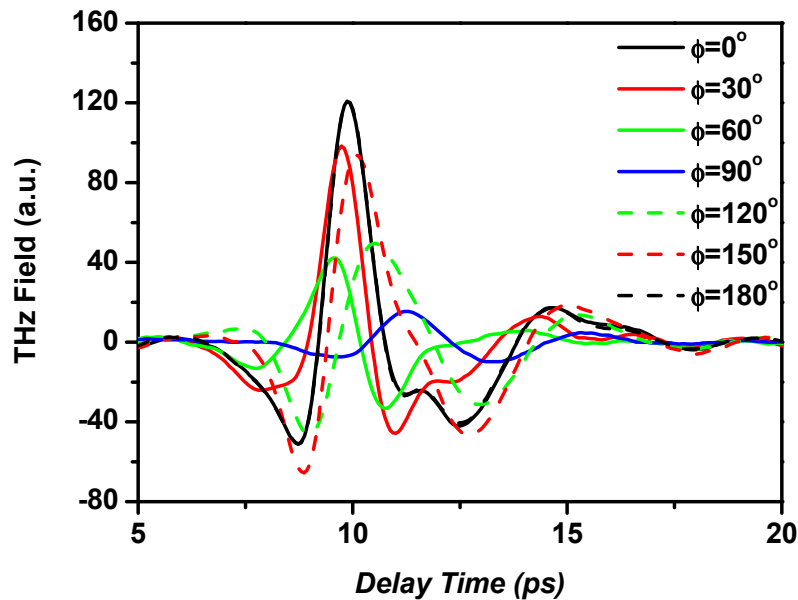
Fig. 2. The temporal waveforms of the THz pulse transmitted through the tunable achromatic quarter wave plate with the E7 layer aligned at magnetic inclination angle $\theta = 0°$ with different rotating angles ϕ are shown together. Here we just show the temporal waveforms at $\phi = 0°$, 30°, 60°, 90°, 120°, 150°, and 180°.

In Fig. 3, the transmittance values with different ϕ (when $\theta = 0°$) are drawn with theoretic prediction at the frequency of 0.44 THz. The main reason we picked up 0.44 THz is the strongest resonant frequency of the THz radiation from PCA-based THz-TDS which is situated there. In other words, the signal-to-noise ratio at 0.44 THz showed the best performance compared with other frequencies. Considering the heavy loss from the LC retarders, we finally decided to show the case of 0.44 THz.
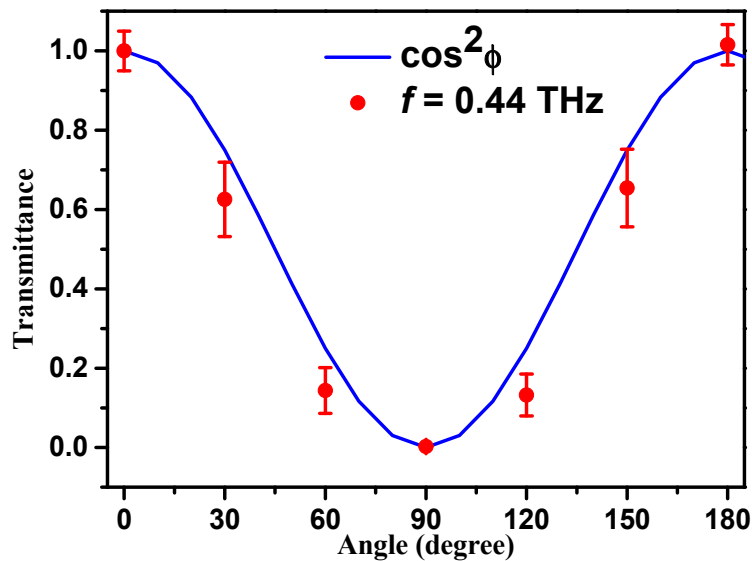

Fig. 3. The transmittance values with different ϕ (when $\theta = 0°$) are drawn together with theoretic prediction at frequency of 0.44 THz.

The experimental retardations obtained with the combination of the three LC plates at $\theta =$ 0° and 30°, depicted in Figs. 4 and 5, respectively.

In Fig. 4, the phase retardation of this device is about 90° from 0.20 to 0.50 THz, when θ = 0°. On the other hand, in Fig. 5, the phase retardation of this device is about 90° from 0.30 to 0.70 THz, when θ = 30°. The operation frequency range can be shifted by rotating the magnet set. The experimental data and the theoretical curves from the calculation of Jones matrices are in very good agreements. The thickness of the LC layer for the THz device should be close to the THz wavelength scale, around hundred μm, which will cause that LC molecules in the middle of cell cannot be aligned well by the magnetic field. The slight deviation between the numerical and the experimental results comes from here.
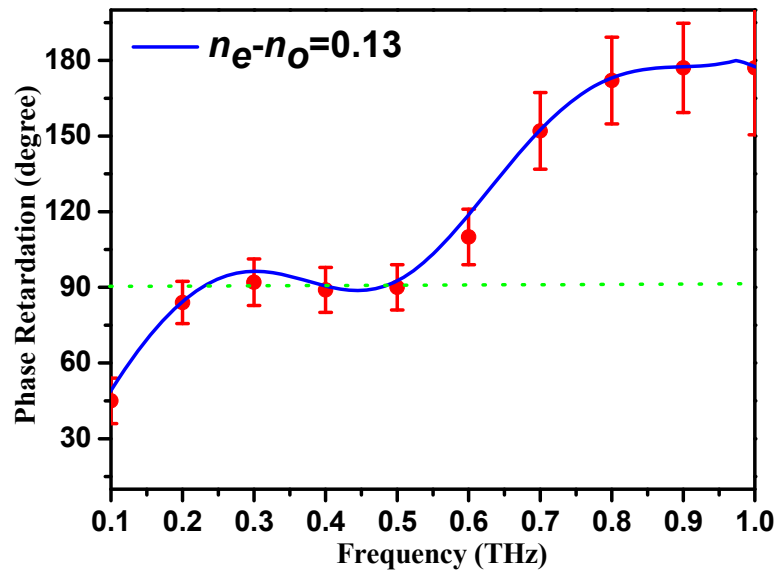

Fig. 4. The phase retardation of this device is about 90° from 0.20 to 0.50 THz, when θ = 0°.

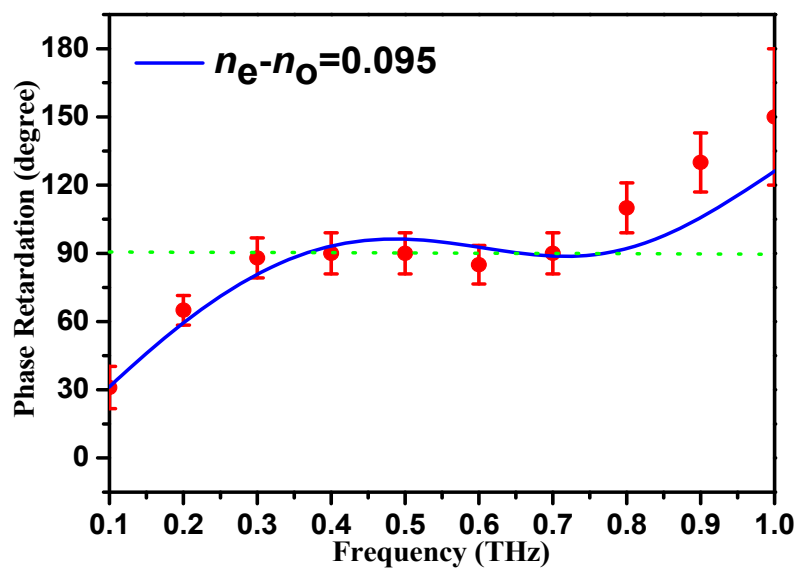Fig. 5. The phase retardation of this device is about 90° from 0.30 to 0.70 THz, when θ = 30°.

Dynamic responses of the devices are also of interests. The response time of the field-off state depended only on the material properties and cell thickness. Because of the slow responses, the current device is not suitable for applications that require fast modulation. However, the device is appropriate for instrumentation or apparatuses that require.

4. Conclusions

In summary, we have demonstrated for the first time an achromatic tunable terahertz (THz) birefringence quarter-wave plate using liquid crystal (LC) cells as the birefringent elements. The phase retardation of this device is 90° ± 9° from 0.20 to 0.50 THz, and the operation range can be tuned to from 0.30 to 0.70 THz by applying magnetically controlled birefringence in three nematic LCs retarders. The insertion loss of the present device is about 8 dB. The experimental data are in good agreements with theoretical predictions. To achieve the much larger bandwidth in THz frequency range, one can extend the design to a combination of more wave plates.

Funding

Author contributions

C.-F. H carried out the sample preparation, and optical measurement. C.-S. Y, F.-C. S, and C.-L. P performed theoretical analysis. C.-S. Y and C.-L. P wrote the manuscript with inputs from all authors.

References

1. M. D. Lavrentovich, T. A. Sergan, and J. R. Kelly, "Switchable broadband achromatic half-wave plate with nematic liquid crystals," Opt. Lett. **29**(12), 1411–1413 (2004).
2. A. Saha, K. Bhattacharya, and A. K. Chakraborty, "Achromatic quarter-wave plate using crystalline quartz," Appl. Opt. **51**(12), 1976–1980 (2012).
3. R.-P. Pan, C.-W. Lai, C.-J. Lin, C.-F. Hsieh, and C.-L. Pan, "Achromatic liquid crystal phase plate for short laser pulses," Mol. Cryst. Liq. Cryst. (Phila. Pa.) **527**(1), 65–71 (2010).
4. R. M. A. Azzam and C. L. Spinu, "Achromatic angle-insensitive infrared quarter-wave retarder based on total internal reflection at the Si-SiO$_2$ interface," J. Opt. Soc. Am. A **21**(10), 2019–2022 (2004).
5. C. Delacroix, P. Forsberg, M. Karlsson, D. Mawet, O. Absil, C. Hanot, J. Surdej, and S. Habraken, "Design, manufacturing, and performance analysis of mid-infrared achromatic half-wave plates with diamond subwavelength gratings," Appl. Opt. **51**(24), 5897–5902 (2012).
6. D. M. Mittleman, "Perspective: terahertz science and technology,'" J. Appl. Phys. **122**(23), 230901 (2017).
7. B. Lu, H. Wang, J. Shen, J. Yang, H. Mao, L. Xia, W. Zhang, G. Wang, X.-Y. Peng, and D. Wang, "A high extinction ratio THz polarizer fabricated by double-bilayer wire grid structure," AIP Adv. **6**(2), 025215 (2016).
8. C.-S. Yang, T.-T. Tang, P.-H. Chen, R.-P. Pan, P. Yu, and C.-L. Pan, "Voltage-controlled liquid-crystal terahertz phase shifter with indium-tin-oxide nanowhiskers as transparent electrodes," Opt. Lett. **39**(8), 2511–2513 (2014).
9. C.-S. Yang, T.-T. Tang, R.-P. Pan, P. Yu, and C.-L. Pan, "Liquid crystal terahertz phase shifters with functional indium-tin-oxide nanostructures for biasing and alignment," Appl. Phys. Lett. **104**(14), 141106 (2014).
10. C.-S. Yang, C. Kuo, P.-H. Chen, W.-T. Wu, R.-P. Pan, P. Yu, and C.-L. Pan, "High-transmittance 2π electrically tunable terahertz phase shifter with CMOS-compatible driving voltage enabled by liquid crystals," Appl. Sci. (Basel) **9**(2), 271 (2019).
11. C.-S. Yang, C. Kuo, C.-C. Tang, J. C. Chen, R.-P. Pan, and C.-L. Pan, "Liquid-crystal terahertz quarter-wave plate using chemical-vapor-deposited graphene electrodes," IEEE Photon. J. **7**(6), Article#: 2200808 (2015).
12. S. F. Zhou, L. Reekie, Y. T. Chow, H. P. Chan, and K. M. Luk, "Phase-shifted fiber Bragg gratings for terahertz range," IEEE Photonics Technol. Lett. **24**(20), 1875–1877 (2012).
13. C.-J. Lin, Y.-T. Li, C.-F. Hsieh, R.-P. Pan, and C.-L. Pan, "Manipulating terahertz wave by a magnetically tunable liquid crystal phase grating," Opt. Express **16**(5), 2995–3001 (2008).
14. B. Mirzaei, J. R. G. Silva, Y. C. Luo, X. X. Liu, L. Wei, D. J. Hayton, J. R. Gao, and C. Groppi, "Efficiency of multi-beam Fourier phase gratings at 1.4 THz," Opt. Express **25**(6), 6581–6588 (2017).

15. C.-L. Pan, C.-J. Lin, C.-S. Yang, W.-T. Wu, and R.-P. Pan, "Liquid-Crystal-Based Phase Gratings and Beam Steerers," Chapter 10, in "Liquid Crystals - Recent Advancements in Fundamental and Device Technologies," InTech Open, London, UK (2018).
16. B. Zhang and Y. Gong, "Achromatic terahertz quarter waveplate based on silicon grating," Opt. Express **23**(11), 14897–14902 (2015).
17. J.-B. Masson and G. Gallot, "Terahertz achromatic quarter-wave plate," Opt. Lett. **31**(2), 265–267 (2006).
18. J. Ornik, L. Gomell, S. F. Busch, M. Hermans, and M. Koch, "High quality terahertz glass wave plates," Opt. Express **26**(25), 32631–32639 (2018).
19. Y.-Y. Ji, F. Fan, X.-H. Wang, and S.-J. Chang, "Broadband controllable terahertz quarter-wave plate based on graphene gratings with liquid crystals," Opt. Express **26**(10), 12852–12862 (2018).
20. C.-Y. Chen, C.-F. Hsieh, Y.-F. Lin, R.-P. Pan, and C.-L. Pan, "Magnetically tunable room-temperature 2 π liquid crystal terahertz phase shifter," Opt. Express **12**(12), 2625–2630 (2004).
21. C.-S. Yang, C.-J. Lin, R.-P. Pan, C. T. Que, K. Yamamoto, M. Tani, and C.-L. Pan, "The complex refractive indices of the liquid crystal mixture E7 in the terahertz frequency range," J. Opt. Soc. Am. B **27**(9), 1866–1873 (2010).
22. F. J. Kahn, "Orientation of liquid crystals by surface coupling agents," Appl. Phys. Lett. **22**(8), 386–388 (1973).
23. P. G. de Gennes and J. Prost, "The Physics of Liquid Crystals", 2nd ed. (Oxford, New York, 1983), Chap. 3.
24. C.-S. Yang, M.-H. Lin, C.-H. Chang, P. Yu, J.-M. Shieh, C.-H. Shen, O. Wada, and C.-L. Pan, "Non-Drude behavior in indium-tin-oxide nanowhiskers and thin films investigated by transmission and reflection THz time-domain spectroscopy," IEEE J. Quantum Electron. **49**(8), 677–690 (2013).